



AD-A283 533



**AIAA-94-2710  
Compliant Metal Enhanced Convection  
Cooled Reverse-Flow  
Annular Combustor**

M. D. Paskin  
Allison Engine Co.  
Indianapolis, IN

W. A. Acosta  
Vehicle Propulsion Directorate  
U.S. Army Research Laboratory  
NASA Lewis Research Center  
Cleveland, OH

**DTIC**  
ELECTE  
AUG 10 1994  
**S G D**

94-25182



*2098*



94 8 09 07 6

**30th AIAA/ASME/SAE/ASEE Joint  
Propulsion Conference**

June 27-29, 1994 / Indianapolis, IN

NASA  
Technical Memorandum 106626  
AIAA-94-2710

Army Research Laboratory  
Memorandum Report ARL-MR-151

# Compliant Metal Enhanced Convection Cooled Reverse-Flow Annular Combustor

Marc D. Paskin  
*Allison Engine Co.*  
*Indianapolis, Indiana*

and

Waldo A. Acosta  
*Vehicle Propulsion Directorate*  
*U.S. Army Research Laboratory*  
*Lewis Research Center*  
*Cleveland, Ohio*

Prepared for the  
30th Joint Propulsion Conference  
cosponsored by AIAA, ASME, SAE, and ASEE  
Indianapolis, Indiana, June 27-29, 1994



National Aeronautics and  
Space Administration



Trade names or manufacturers' names are used in this report for identification only. This usage does not constitute an official endorsement, either expressed or implied, by the National Aeronautics and Space Administration.

# COMPLIANT METAL ENHANCED CONVECTION COOLED REVERSE-FLOW ANNULAR COMBUSTOR

Marc D. Paskin  
Allison Engine Co.  
Indianapolis, IN

and

Waldo A. Acosta  
U. S. Army Vehicle Propulsion Directorate (ARL)  
Lewis Research Center  
Cleveland, OH

Accession For	
NTIS CRA&I	<input checked="" type="checkbox"/>
DTIC TAB	<input checked="" type="checkbox"/>
Unannounced	<input type="checkbox"/>
Justification .....	
By .....	
Distribution / .....	
Availability Codes	
Dist	Avail and/or Special
A-1	20

## Abstract

A joint Army/NASA program was conducted to design, fabricate, and test an advanced, reverse-flow, small gas turbine combustor using a compliant metal enhanced (CME) convection wall cooling concept. The objectives of this effort were to develop a design method (basic design data base and analysis) for the CME cooling technique and then demonstrate its application to an advanced cycle, small, reverse-flow combustor with 3000°F (1922 K) burner outlet temperature (BOT). The CME concept offers significant improvements in wall cooling effectiveness resulting in a large reduction in cooling air requirements. Therefore, more air is available for control of burner outlet temperature pattern in addition to the benefits of improved efficiency, reduced emissions, and smoke levels. Rig test results demonstrated the benefits and viability of the CME concept meeting or exceeding the aerothermal performance and liner wall temperature characteristics of similar lower temperature-rise combustors, achieving 0.15 pattern factor at 3000°F (1922 K) BOT, while utilizing approximately 80% less cooling air than conventional, film-cooled combustion systems.

## Introduction

Throughout the gas turbine industry, research effort is being directed at improving the performance, emissions and reliability of gas turbine engines while reducing the specific fuel consumption. Higher cycle efficiencies can be realized if the cycle pressure ratio and turbine inlet temperatures are raised along with increasing individual component efficiencies. The higher operating pressure and temperatures require that a greater portion of the combustor throughflow air be

used for burning the fuel in the primary zone, thus leaving less air for cooling the liner walls. Conventional wall cooling methods (e.g., film cooling) are incapable of providing satisfactory durability without using excessive amounts of cooling air, which, in turn, severely restricts air available for temperature pattern control. Engine envelope demands further exacerbate the situation by requiring foldback (reverse-flow) combustor designs, which reduce engine length and weight but contain an inherently large combustor surface area-to-volume ratio. Therefore, to meet one of the most critical needs of future small gas turbine engine designs<sup>1</sup>, advanced wall cooling techniques are required to minimize cooling air requirements.

Many advanced cooling schemes have been developed in recent years<sup>2</sup> and include enhanced convection film cooling techniques such as etched convective channels, impingement, multiple discrete holes (effusion) and transpiration (Lamilloy<sup>®</sup>) cooling. In addition, there has been a recent rapid growth in research and development effort aimed at introducing ceramics into gas turbine engines.

Ceramic coatings are used extensively as thermal barrier coatings in gas turbine engines. High temperature ceramic coatings protect the metal substrate from the combined effects of temperature and oxidation-corrosive environment. The effectiveness of a ceramic thermal barrier increases with ceramic thickness and porosity. Ceramic coating thickness are limited to 0.010 - 0.030 in. (0.0254 - 0.0762 cm) in environments where rapid thermal excursions subject the ceramic to severe thermal shock.

\* Lamilloy<sup>®</sup> is a registered trademark of the Allison Engine Co.

The compliant metal enhanced (CME) convection concept, one of the most effective cooling schemes, was developed jointly by the U.S. Army and NASA Lewis Research Center.<sup>3,4,5,6</sup> This cooling scheme uses a sintered metal fiber structure between a thick ceramic barrier coating (TBC) and a high temperature alloy substrate as shown in Figure 1. The intermediate fiber metal pad is designed to yield at relatively low levels of stress, thereby absorbing the differential expansion which develops between the metal substrate and ceramic as the material is heated. This thermal barrier design approach offers superior properties because the fiber metal strain isolator in itself is an excellent insulator.

Current film cooling technology addresses small turbine engine cycles operating with moderate pressure ratios and BOT's less than 2500°F (1644 K). The CME combustor was designed for an advanced small gas turbine engine cycle with a 19:1 pressure ratio or higher and 3000°F (1922 K) BOT. Table I provides the design conditions for the CME combustor. At the severe conditions of the design point, the CME concept offers more than 80% reduction in the required coolant flux compared to conventional film cooling.<sup>3</sup>

This paper describes the results of the burner rig tests. It includes characterization of cold pressure drop, lean blow-out and ignition mapping, steady-state performance throughout the operating range to 3000°F (1922 K) BOT as well as two series of simulated cyclic thermal shocks at BOT's of up to 2700°F (1755 K) (32 total cycles) and 3000°F (1922 K) (68 cycles). Rig test results demonstrated the benefits and viability of the CME concept meeting or exceeding the aerothermal performance and liner wall temperature characteristics of similar lower temperature-rise combustors.

## Combustion System

### Overview of Combustion System

The combustor selected was a compact, annular, reverse-flow design incorporating a single row of primary holes and a single row of dilution holes on both the inner and outer liners. The CME concept was used in the construction of the inner and outer liner walls as well as the outer transition liner (OTL). The dome was effusion cooled and contained 12 piloted-air blast fuel nozzles each surrounded by an axial swirler. Design point operating conditions are given in Table I. Figure 2 shows the CME combustor predicted airflow distribution at the design point.

Table I  
Combustor design conditions.

### CMC combustor

Wa (liner flow, lb/s)	7.940
P3 (inlet pressure, psia)	271
T3 (inlet temperature, °F)	895
Wf (fuel flow, lb/hr)	1008
F/A (fuel/air ratio)	0.03526
Wcorr (corrected flow, lb/sec)	0.696
Temperature rise (°F)	2105
Burner outlet temperature (°F)	3000
Liner pressure drop (%)	5

## Combustor Design Procedure

### Optimization of Wall Isolated Segment Design

The coolant orifice diameter and spacing, ceramic "tile" side length, exit slot width, and ceramic thickness were the critical CME wall design parameters requiring optimization. Preliminary and final design of the wall were carried out during the Task II and Task III efforts. Details of the development of the basic data base and analysis methodology for determining coolant flux, pressure drop, and wall temperatures in the CME structure can be found in References 7 and 8.

A tile consisted of a single square element of ceramic with cooling air fed through a single orifice in the substrate. The air enters the porous pad through the orifice and flows around the backside of the ceramic and exits through the slots between the tiles. A 2-D heat transfer model was used to predict wall temperature as a function of tile side length for individual tile segments. A nominally square tile shape was selected and the pattern fixed by the choice of primary and dilution orifices located on the exit slots between tiles. The 2-D model wall temperature predictions for an arbitrary coolant orifice diameter were used to scale the proper hole diameter to achieve a ceramic/metal interface temperature with margin under the 1750°F (1228 K) design limit. Calculation of the cooling orifice dimension allowed the use of the flow model to calculate a single tile flow rate, which was summed for all tiles to determine the overall coolant flow for the combustor. After the cooling circuit was determined, extensive heat transfer calculations were carried out to optimize the design for 3000°F (1922 K) BOT. Final design results predicted that the critical CME ceramic/metal interface temperatures peak at approximately

1400°F (1033 K) at most locations within the combustor and that the axial temperature gradients would be small.

### Optimization of Overall Combustor Aerothermal and Mechanical Design

Final optimization of the combustor design was carried out with the 3-D combustor performance analysis model COM3D. The output included velocity vectors, contours of gas temperature, fuel-air-ratio ( $f/a$ ), mass fraction unburned fuel as well as average gas temperatures and  $f/a$  ratios over user defined combustor subvolumes. The COM3D output was used as input to the pseudo 3-D heat transfer code, WALL3D, which gave wall temperature predictions as a function of axial and circumferential location.

The combustor was simulated by modeling a single fuel nozzle 30 degree sector. The fuel nozzle-swirler boundary condition of the dome was represented as a three swirler arrangement accounting for the two fuel nozzle swirlers and the dome axial swirler. Other boundary conditions included the specification of operating conditions and airflow distribution. Control parameters, convergence criteria, parameters for the turbulence submodel, and input for subvolume, hybrid empirical performance, and 3-D heat transfer model made up the balance of the required input database.

Figure 3 shows the velocity vector profile through the fuel nozzle centerline from the 3-D analysis of the final design. A well balanced recirculation zone and well behaved, radially oriented primary jets impinging near the center of the combustor were observed. The effects of this flowfield on temperature contours is shown in Figure 4.

In general, the temperature contours revealed a well behaved primary zone with the hottest gases contained in the interior between the dome and the primary jets, where the recirculation zone is well defined. The temperature fields also indicated good uniformity of the gas temperatures downstream of the dilution jets where rapid quenching of the hot primary zone gases occurs due to the evidence of uniform mixing.

The subvolume averaged data from the completed 3-D aerothermal analysis was subsequently used to run the pseudo 3-D heat transfer model (WALL3D) and provide input for the Allison empirical correlation analysis for combustor performance prediction.

Predicted 3-D wall temperatures for the 3000°F (1922 K) BOT design condition are shown in Figure 5 for both the inner and outer walls for the CME combustor. The substrate surface temperatures range from 1100°F (867 K) to 1300°F (978 K). The results also revealed that the combustor met the design 1750°F (1228 K) ceramic/Brunsbond<sup>†</sup> interface temperature goal. The predicted interface temperatures peaked at just over 1550°F (1117 K) near the entrance to the outer transition liner. Most other axial locations on both the inner and outer walls ranged from 1430 (1050) to 1480°F (1078 K) and agreed acceptably well with the 2-D finite difference heat transfer analyses.

The final analysis of the CME combustor used the Allison empirical correlation code to predict performance based on the subvolume average data from the COM3D 3-D simulation. The results given in Table II show high combustion efficiency, good pattern factor, low unburned hydrocarbons (UHC) and carbon monoxide (CO), but high smoke. The relatively high smoke of these predictions was unexpected and may be related to the density of specified subvolumes in the COM3D input or to inaccuracies in the correlation constants for these parameters. Overall the predicted wall temperatures and combustor performance indicated an acceptable design.

Following optimization of the combustor aerothermal design, mechanical design and preparation of detail drawings were completed. Fabrication of the combustor followed.

### Experimental Results and Analysis

#### Description of Test Facility and Capability

Full scale rig tests were performed to determine combustion steady-state performance, ignition,

Table II  
Summary of results from 3-D performance code prediction.

NO <sub>x</sub> (E.I.)	39
CO (E.I.)	0.41
UHC (E.I.)	0.16
Smoke No. (SAE)	26
Combustor efficiency, $\eta_c$ (%)	99.4
Pattern factor	0.176

<sup>†</sup> Trademark, Technetics Corporation, DeLand, FL

lean stability limits, exhaust emissions, and temperature levels and gradients. Combustor structural durability was assessed by conducting cyclic thermal shock tests.

The combustor rig simulated an engine flow path from compressor diffuser to the inlet of the gasifier turbine. The rig had provision to extract bleed air to simulate engine operation. Rig airflows were measured with ASME thin plate orifices. Instrumentation throughout the rig provided overall performance measurements of the test combustor. A feature of the rig was the rotating probe for measuring burner outlet temperature. Eight platinum-platinum-rhodium thermocouples were air cooled and mounted on four air-cooled platinum bodied rakes offset 90 degrees. Temperatures were correlated with uncooled, reference thermocouples which provided the approximate 3100°F (1978 K) bulk average BOT capability of the rig. A platinum bodied total pressure rake along with a static pressure tap were also mounted on the rotating probe. There were four stationary emissions probes at the exit of the combustor. Twenty chromel-alumel thermocouples were attached to the combustor to measure temperatures throughout the CME wall. As shown in Figures 1 and 2, the thermocouples were placed on the effusion-cooled dome, on the substrate surface (cold side), on the interfaces between ceramic and compliant layer, and the compliant layer and substrate for the inner, outer and OTL liners. Combustor inlet conditions were measured with 14 total pressure rakes. In addition, there were 16 static pressure taps throughout the combustor rig. Two Flotron transducers were installed in series to measure fuel flow. Cooling water was used to cool the emission probes and to quench the exhaust gases upstream of the exhaust valve as well as the exhaust spool.

### Test Procedures

Cold flow pressure drop characteristics were determined by setting the rig to a given pressure, temperature, and airflow and then recording the pressure drop. Pressure drops were measured over a range of corrected flows.

High pressure combustion tests were carried out after cold flow pressure evaluation. The combustor was fired and stabilized at simulated engine power conditions from idle to maximum power. For each condition the rig operating parameters (i.e. airflow, pressure, temperature, and emissions) were measured. The BOT's were measured by rotating the BOT probe while continuously recording thermocouple output. The probe was rotated at approximately 0.40 inch per second. This speed

allowed the thermocouple elements to fully respond to the gas path temperature. At the conclusion of each combustion test, the fuel nozzles were purged with high-pressure nitrogen to prevent fuel carboning in the nozzle passages.

Ignition tests were performed by setting flow conditions for a given operating point and then initiating a preset fuel flow. Ignition must be obtained within one or two seconds of reaching full fuel manifold pressures. The test was repeated at the same flow condition until the minimum fuel flow for a successful ignition was obtained.

Lean blowout fuel/air ratios were determined by setting flow conditions for a given operating point and slowly reducing fuel flow until no flame can be detected by the outlet thermocouples. Fuel flow was then increased to ensure that the combustor had blown out and would not relight.

Smoke and gaseous emissions were measured at sea-level standard day steady-state operating conditions from idle to maximum power. Smoke is important for visibility considerations and the gaseous emissions CO, UHC, and NO<sub>x</sub> are important for calculating combustion efficiency and for air pollution considerations. Smoke was measured in accordance with SAE ARP-1179(9) and gaseous emissions in accordance with SAE ARP-1256.(10)

Cyclic thermal shock tests were performed to assess the durability of the CME combustor. The tests were carried out by holding burner inlet conditions of pressure, temperature, and airflow constant while repeating fuel flow excursions between minimum, determined to avoid flameout, and a maximum to achieve a BOT of either 2700°F (1756 K) (initial tests) or 3000°F (1922 K) (final test).

### Test Plan

The overall objective of the test plan was to establish the cooling effectiveness, performance, and durability of the CME combustor concept. Five test builds and approximately thirty (30) hours of combustion testing were planned. The test conditions are given in Table III. Lean blowout points are designated LBO, ignition points are designated IGN, and steady-state points, SS. All cold flow testing was performed at ambient conditions over a range of corrected flows from 0.27 to 0.75 lb/s with bleed air off. Table IV describes the cyclic test program. Figure 6

provides a single cycle illustration for the throttle excursions of cyclic tests 1 through 3.

### Test Results and Analysis

The test program was accomplished in five rig builds (BU-1 through BU-5). A build is defined as a combustion test involving assembly of the combustor, instrumentation, and rig followed by teardown inspection of the combustor rig to assess condition. The five builds are summarized as follows:

- BU-1 - Initial steady-state (SS) performance evaluation covering idle condition (point 4 in Table III) through MCP (operating point 12 in Table III).

- BU-2 - Dedicated 2800°F (1811 K) BOT thermal paint test.
- BU-3 - Ignition/lean blowout (LBO) mapping, SS performance up to 3000°F (1922 K).
- BU-4 - Cyclic thermal shock testing at a BOT of 2700°F (1756 K) (32 total cycles).
- BU-5 - Cyclic thermal shock testing at a BOT of 3000°F (1922 K) (68 total cycles).

### BU-1

The measured cold flow pressure drop was 4.5% at the design point corrected flow (0.696 lb/sec) compared to a predicted value of 5%, as shown in Figure 7. With good agreement from the cold flow tests, combustion tests were initiated. A photograph of the liner showing the after-test

Table III.  
Matrix of test conditions for CME combustor.

Point	Condition*	BIP (psia)	BIT (°F)	Rig flow (lbm/s)	Blade bleed (lbm/s)	Vane bleed (lbm/s)	Liner airflow (lbm/s)	Fuel flow	F/A	BOT (°F)	Vr, corr (ft/s)	Wcorr (lbm/s)
1 (LBO)	6 KM 72.5 KCAS Cold day idle	35.9	229	1.73	0.07	0.14	1.52	68.5	0.0125	1112	73.7	0.717
2 (LBO)	6 KM 0.6 MN Cold day idle	41.2	259	2.08	0.09	0.16	1.83	65.6	0.01	973	96.6	0.768
3 (LBO)	3 KM 0.3 MN ISA idle	46.3	370	2.10	0.09	0.17	1.84	89.9	0.0136	1307	129.4	0.739
4 (LBO)	SLS ISAA idle	61.8	414	2.70	0.12	0.21	2.37	127	0.0149	1460	184.8	0.731
5 (LBO)	6 KM 0.3 MN Cold day decel	68.7	468	3.22	0.14	0.25	2.83	85.6	0.0084	1056	248.8	0.810
6 (IGN)	SLS 59°F day 10% NGG	14.9	65	0.27	0	0	0.27	--	--	--	7.6	0.268
7 (IGN)	SLS 59°F day 15% NGG	15.3	69	0.41	0	0	0.41	--	--	--	11.7	0.398
8 (IGN)	SLS 59°F day 20% NGG	15.6	74	0.54	0	0	0.54	--	--	--	15.7	0.516
9 (IGN)	SLS 59°F day 25% NGG	16.0	78	0.68	0	0	0.68	--	--	--	20.1	0.636
10 (IGN)	SLS 59°F day 30% NGG	16.3	83	0.81	0	0	0.81	--	--	--	24.4	0.747
11 (SS)	50% IRP	181.3	717	6.73	0.29	0.53	5.91	494	0.0232	2148	836	0.722
12 (SS)	MCP	235	819	8.21	0.35	0.65	7.21	720	0.0277	2475	1204	0.708
13 (Cyclic)	IRP	261	873	8.82	0.38	0.70	7.74	831	0.0298	2701	1404	0.699
14 (SS)	TP1 (thermal paint)	272	895	9.04	0.39	0.71	7.94	927	0.0324	2800	1488	0.693
15 (SS, cyclic)	TP2 (thermal paint - max. power)	272	895	9.04	0.39	0.71	7.94	1008	0.0353	3000	1488	0.693

- \* KM = altitude in kilometers
- MN = Mach number
- SLS = sea level, static condition
- NGG = gas generator speed
- IRP = intermediate rated power
- MCP = maximum continuous power

Table IV.  
Cyclic testing program for CME combustor.

<u>Condition</u>	<u>Point number</u>	<u>Burn hours</u>	<u>Number of cycles</u>	<u>Approximate average</u>		<u>Teardown/inspection rebuild</u>
				<u>Max. (°F) BOT</u>	<u>Min. (°F) BOT</u>	
IRP (1)	13	3.0	32	2700	1300	Yes
TP2 (2)	15	6.5	92	3000	1300	No
TP2 (3)	15	6.5	91	3000	1300	No

condition is given in Figure 8. As shown, no damage was sustained to the combustor hardware, and the ceramic tiles were in place with no spalling or delamination noted. The only noticeable change, other than discoloration, from the new ceramic condition were small hairline cracks on the OTL innermost two rows of tiles. Further details can be found in Reference 3.

#### BU-2

This build was a dedicated thermal paint test at 2800°F (1811 K). The test provided wall temperature data with poor resolution of isotherms due to the unexpected length of time required to reach the operational point (point TP1, Table III). However, the thermal paint revealed and verified hot spots on the dome and the OTL as well as the necessity to adjust local coolant flux. Rework of the liner dome and OTL was carried out following BU-2 by adding laser drilled effusion cooling holes to the dome and several additional coolant orifices (through the substrate only) on the OTL.

Overall the test went smoothly; however, the test data indicated a high pattern factor relative to the BU-1 test due to a hot streak in the exhaust gas near the hub as well as high wall temperatures on the OTL and dome. However, on the inside and outside liner walls, no hot spots were observed and wall thermocouples indicated outside (cold side) metal temperatures in the 1100 to 1350°F (867 to 1006 K) range.

The pattern factor was measured as 0.218 compared to the 0.150 value obtained during the BU-1 test. Combustion efficiency, pressure drop, and emissions were acceptable and in-line with previous measurements. The main concern with BU-2 test results were the dome and OTL wall temperature measurements and the streaky condition of the circumferential BOT trace.

The OTL, which also utilizes the CME wall construction ran with much hotter wall temperatures (approximately +200°F (367 K) at the ceramic-Brunsbond interface) than either the inner or outer liner. Flow testing evaluation of the OTL, isolated from the rest of the combustor, was later carried out and indicated a 67% reduction in coolant flux relative to the design goal. Differences in the required fabrication process for the OTL, compared to the inner and outer liner, are the cause of this blockage and indicate the necessity to adjust the design method or improve the manufacturing process for the OTL.

Exhaustive investigation of the cause of the hot streak and cold spikes did not yield a conclusive cause. The best conclusion, based on review of the data, was that an air leak occurred near the inner liner-rig seal interface and was possibly related to improper rig assembly. In addition, to rule out effects from the air-cooled BOT thermocouple probes, BU-3 test plans were modified to include combustor operation at the BU-1 condition (point 12, MCP, Table III), with and without thermocouple probe cooling air active.

Figure 9 provides the overall CME combustor airflow distribution following rework. Comparison with Figure 2 shows cooling flow for the dome and OTL was increased by more than 2% each and the total effective area of the liner has been increased by nearly 0.1 in<sup>2</sup>.

#### BU-3

After rework of the combustor dome and OTL to increase local coolant flux, cold flow pressure drop tests were carried out. At the design point corrected flow of 0.696 lb/sec, the measured liner pressure drop was 4.2% compared to the predicted value of 4.5%. With acceptable agreement, LBO and ignition tests were initiated.

Results of the LBO test are presented in Figure 10, and ignition test results are provided in Figure 11. For the LBO tests, a comparison is made to measured data for the combustion system for which the CME combustor was derived. CME combustor LBO results correlated well with the reference velocity parameter,  $V_r \delta \theta$ . However, the data lie slightly above the stability curve for the combustion system for which the CME combustor was derived. LBO results are still considered acceptable, ranging from 0.004 to 0.007 fuel/air ratio over the operating conditions of interest. LBO test points were previously described in Table III.

Ignition data presented in Figure 11, correlated well with corrected reference velocity and is observed to closely parallel previous experience. Recorded ignition was slightly higher than expected, ranging from 0.04 at low velocity to about 0.025 at the high corrected reference velocity.

As reported, the BU-2 2800°F (1811 K) BOT performance data showed a poor pattern factor and circumferential exit temperature data indicating an air leak. Therefore, the test plan was modified to include steady-state operating points that would repeat the BU-1 test condition of approximately 2400°F (1589 K) BOT. In addition, this point was run back-to-back with and without thermocouple probe cooling air applied. Data from the test showed that the air leakage was eliminated with the new build and that performance of the CME combustor, with the probe cooling air off, repeated the BU-1 data. Steady-state performance tests were also carried out at temperatures up to 3000°F (1922 K) BOT. Pattern factor at this condition was 0.15 with acceptable radial profile. Based on these encouraging results, it was concluded that the misleading BU-2 temperature distributions were caused by an air leak related to rig assembly. In addition to pattern factor and radial profile, pressure drop, combustion efficiency, emissions, and smoke results were acceptable and comparable to BU-1 results.

During BU-3, steady-state performance of BU-2 was repeated (2800°F (1811 K) BOT) and then the maximum power condition was run at 3000°F (1922 K).

The circumferential and radial BOT traces for the 2800°F (1811 K) condition are provided in Figures 12 and 13, and for the 3000°F (1922 K) BOT condition in Figures 14 and 15. Review of the data indicates liner pressure drop falls directly on the predicted line for the post re-worked combustor. At

the corrected flow of 0.680 - 0.695, the measured liner pressure drop was 4.7 to 5.0%. Pattern factor was calculated as 0.130 for the 2800°F (1811 K) BOT condition (compared to 0.218 for BU-2) and 0.156 at the 3000°F (1922 K) condition. Radial profile was consistent with the acceptable results obtained during previous testing.

Wall thermocouple measurements were very favorable and continued to indicate the effectiveness of the CMC cooling scheme.

The wall thermocouple temperature measurements of the 3000°F (1922 K) BOT condition can be compared to the predictions given in Figure 5. The predicted metal surface temperatures range from 1100 to 1300°F (867 to 978 K) compared to 1124°F (880 K) measured average for the outer wall and 1388°F (1027 K) measured average for the inner wall. At the critical ceramic/Brunsbond interface, predicted temperatures range from 1430°F (1050 K) to about 1500°F (1089 K) compared to and average measured outer wall temperature of 1264°F (958 K). The average measured inner wall temperature at the ceramic/compliant layer interface was not available because of failed thermocouples in two (2) locations.

However, the design coolant flow distribution appears to be adequate based on wall thermocouple measurements that were available.

#### BU-4

The durability of the CME cooling concept was evaluated in a series of cyclic tests. The first consisted of a 3-hr, 32 cycle thermal shock test at a maximum BOT of 2700°F (1756 K). The specific cycle is given in Figure 6. The 32 cycle test was completed without incident and inspection of the combustor and OTL revealed no apparent damage or deterioration.

Photos of the liner and OTL following the 2700°F (1756 K) BOT cyclic test are shown in Figures 16 and 17, respectively. Overall steady-state performance was consistent with other similar test points with the exception of pattern factor. Before initiation of cyclic testing, pattern factor was measured as 0.197 and increased to 0.226 following the 32nd cycle test. After comparing the BOT traces of BU-4 with BU-2, it appears that the air leak appears to have returned. Hence, a similar value of pattern factor was also obtained. The cause of the leak may be related to rig assembly or possibly mechanical distortion from the severe 3000°F (1922 K) average temperature of BU-3.

Radial profile, emissions, efficiency, and wall temperature results were all similar to previous results. In addition, comparison of before and after steady-state performance, including wall temperature levels, indicated little if any change in CME combustor performance during or after the 32 cycle durability test.

### BU-5

The other phase of the cyclic testing was carried out at 3000°F (1922 K) without incident and with stable operating conditions for 68 cycles.

Steady-state performance measurements were made at the beginning of the test and after 30 cycles. Review of the data indicate, once again, the presence of an air leakage which impacted pattern factor. During BU-5, pattern factor increased to the 0.25 level compared to the 0.20 levels of BU-4. It was suspected that the durability testing of BU-4 exasperated the air leakage problem. After 30 cycles no significant change in combustor operation was observed. Steady-state performance was consistent with previous data at the 3000°F (1922 K) BOT condition.

Figures 18 through 21 provide selected wall thermocouple measurements for the first 67 cycles. Wall temperature levels fluctuate with the fluctuation of operating conditions. All thermocouples maintained relatively steady values up to the 68th cycle. The wall thermocouple readings provide further evidence that the CME combustion system cooling circuit design was adequate to provide acceptable wall temperature levels with a large reduction in coolant flux and operating much more severe than current systems.

During the 68th cycle, as fuel was increased to attain 3000°F (1922 K) BOT condition, a sudden over temperature was observed. Rig inspection revealed that the axial swirler at the No. 4 fuel nozzle position was mechanically displaced. The over temperature caused the inner liner-to-rig seal to melt, which deposited on the OTL as shown in Figure 22. In spite of the severe temperature conditions, the outer liner ceramic tiles survived relatively intact. A view of the outer liner tiles, showing discoloration and through-the-plane cracking is provided in Figure 23. On the other hand, much more damage was sustained to the inner wall tiles where a view is given in Figure 24. This was attributed to the starvation of coolant flow on the inner wall when the swirler failed. Because of the reverse-flow design, inlet air enters at the outer wall and must flow across the combustor dome before turning and entering the inner wall

plenum. With the open area surrounding fuel nozzle 4, it is suspected air would preferentially enter the opening and consequently starve the inner wall of coolant air. This likely exasperated the failure of the inner seal which may have led to the type of mechanical distortion observed around the dome.

Although failure occurred, data analysis indicates until the sudden temperature peak on the 68th cycle, the combustor performance was stable with no observable indications of progressive degradation. Therefore, the CME technology is considered to offer considerable combustor performance benefits and durability characteristics, based on the limited test program, seem positive.

### Summary and Conclusions

A joint U.S. Army/NASA program was conducted to design, fabricate, and test an advanced, reverse flow, small gas turbine combustor utilizing a compliant metal enhanced (CME) convection wall cooling concept. The objectives of this effort were to develop a design method (basic data and analysis) for the CME cooling technique and demonstrate the application for an advanced cycle combustor with 3000°F (1922 K) burner outlet temperature (BOT).

The developed design methodology was applied to the full scale design and the combustor fabricated and tested. In general, rig data were found to be consistent with the design system predictions. Rig test results demonstrated the benefits and viability of the CME concept to meet or exceed the performance of similar combustors, achieving a 0.15 pattern factor at 3000°F (1922 K) BOT while utilizing approximately 80% less cooling air than conventional, film-cooled combustion systems.

Mechanical failure of the axial swirler during cyclic durability testing and subsequent combustor damage was an isolated incident and was unrelated to the performance of the CME wall concept.

### References

1. E. P. Demetri, R.F. Topping, and R.P. Wilson, Jr., "Study of Research and Development Requirements of Small Gas Turbine Combustors," NASA CR-159796, January 1980.
2. D.A. Nealy, S.B. Reider, H.C. Mongia, "Alternate Cooling Configurations for Gas Turbine Combustion Systems," AGARD Conference Proceedings No. 390, 1985, pp. 25-1 to 25-15.

3. M. Paskin, P. Ross, H. Mongia, and W. Acosta, "Composite Matrix Cooling Scheme for Small Gas Turbine Combustors," AIAA Paper No. 90-2158, July 1990.

4. R.R Venkat Raman, G. Roffe, Testing of Felt-Ceramic Materials for Combustor Applications," NASA CR-168103, April 1983.

5. D.B. Ercegovic, C.L. Walker, and C.T. Norgren, "Ceramic Composite Liner Material for Gas Turbine Combustors," AIAA Paper 84-0363, January 1984.

6. W.A. Acosta and C.T. Norgren, "Small Gas Turbine Combustor Experimental Study-Compliant

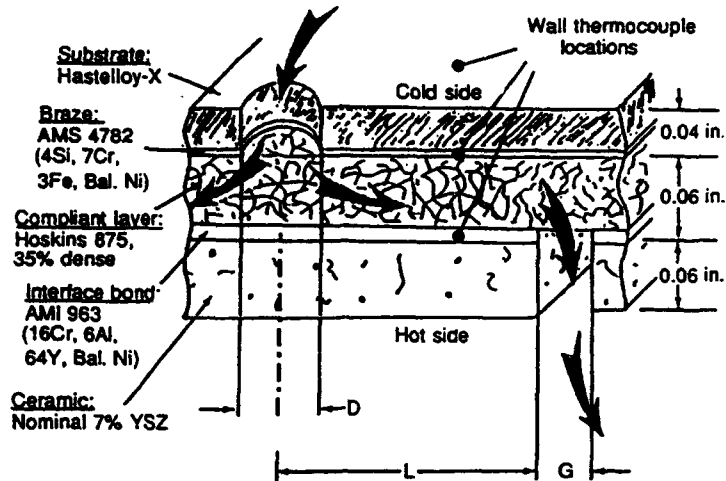
Metal/Ceramic Liner and Performance Evaluation," NASA TM-87304, June 1986.

7. M.D. Paskin, H.C. Mongia, and W.A. Acosta, "An Efficient Liner Cooling Scheme for Advanced Small Gas Turbine Combustors," AIAA Paper 93-1763, June 1993.

8. M.D. Paskin and H.C. Mongia, "Composite Matrix Experimental Combustor," NASA CR-194446, April 1994.

9. "Aircraft Gas Turbine Engine Exhaust Smoke Measurement," SAE ARP-1179, May 1970.

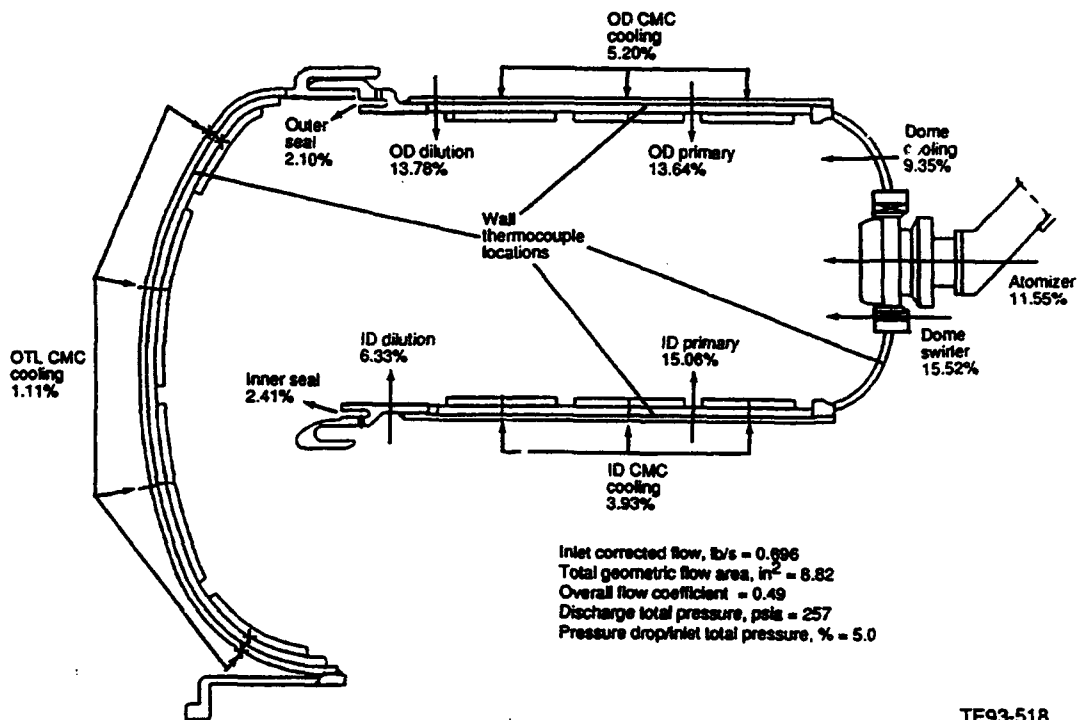
10. "Procedure for the Continuous Sampling and Measurement of Gaseous Emissions from Aircraft Turbine Engines," SAE ARP-1256, Octobre 1971.



- Orifice diameter (D) and spacing, ceramic tile dimension (L) and slot width (G) optimized for combustor and transition liners
- Air inlet orifice effective area =  $Cd(1 - \epsilon)Ah$   
 $Ah = \pi D^2/4$   
 Pad density =  $\epsilon = 0.35$   
 Slot exit geometric area,  $Ae = 2(L + G)^2 - 2L^2$   
 For isolated circular tiles,  $Ae = \pi[(L + G)^2 - L^2]$   
 Exit turning area,  $At = (1 - \epsilon)Ae$

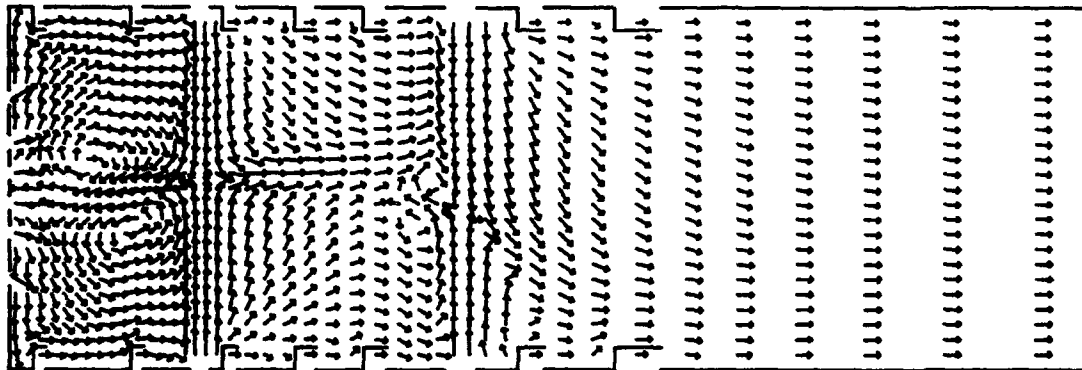
TE90-2475A

Figure 1.—Schematic of compliant metal/ceramic isolated wall segment.



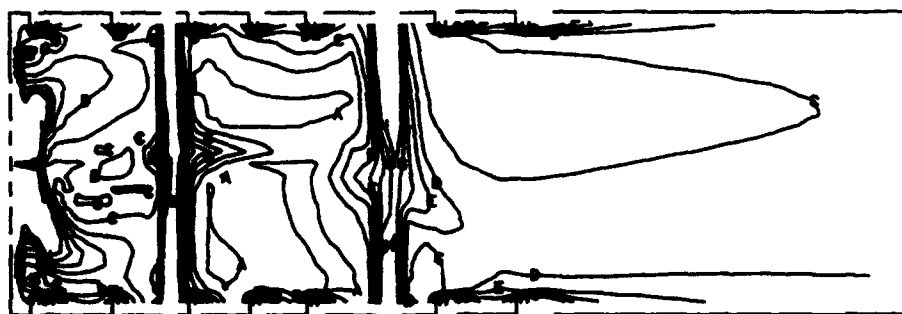
TE93-518

Figure 2.—CME combustor predicted airflow distribution at design point, before rework.



TE93-526

Figure 3.—COM3D velocity vectors, i-j plane, k=16, fuel nozzle centerline.



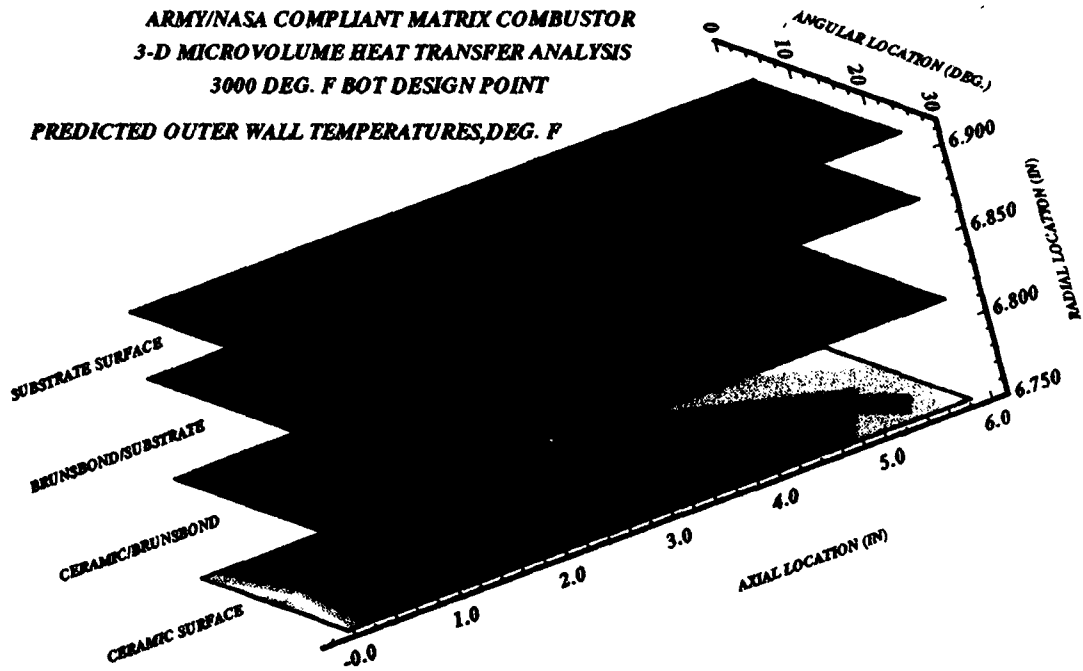
- |        |        |
|--------|--------|
| A 4000 | E 2500 |
| B 3500 | F 2200 |
| C 3000 | G 2000 |
| D 2000 | H 1000 |

TE93-529

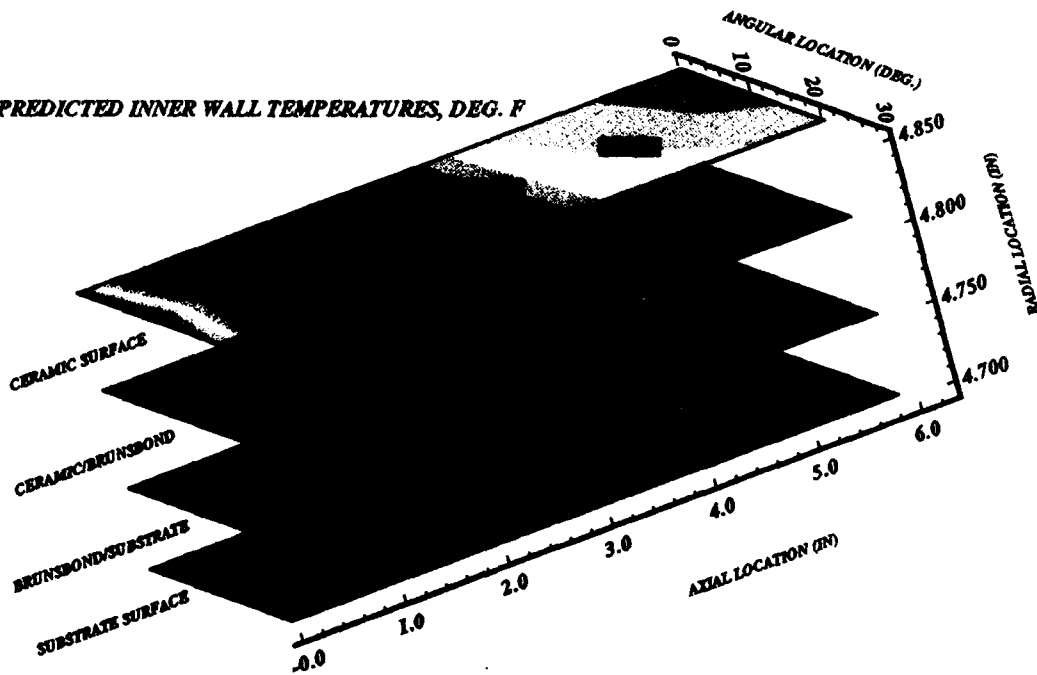
Figure 4.—Temperature contours from COM3D, i-j plane, k=16, fuel nozzle centerline.

ARMY/NASA COMPLIANT MATRIX COMBUSTOR  
3-D MICROVOLUME HEAT TRANSFER ANALYSIS  
3000 DEG. F BOT DESIGN POINT

PREDICTED OUTER WALL TEMPERATURES, DEG. F



PREDICTED INNER WALL TEMPERATURES, DEG. F



TE93-537

Figure 5.—Army/NASA compliant matrix combustor 3-D microvolume heat transfer analysis 3000 °F BOT design point.

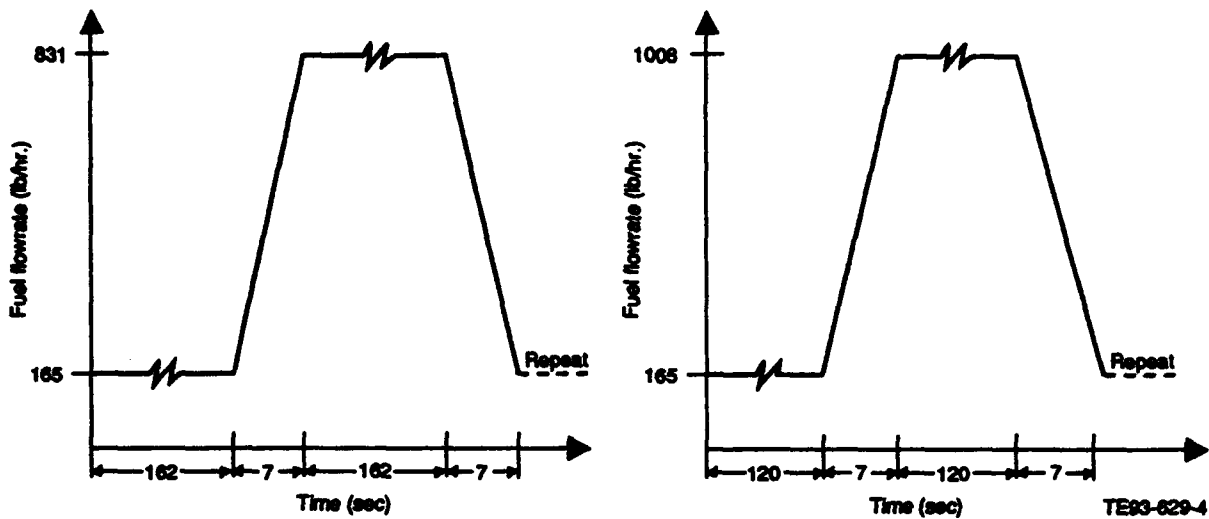


Figure 6.—Single-cycle illustration for throttle excursions of cyclic tests 1 to 3.

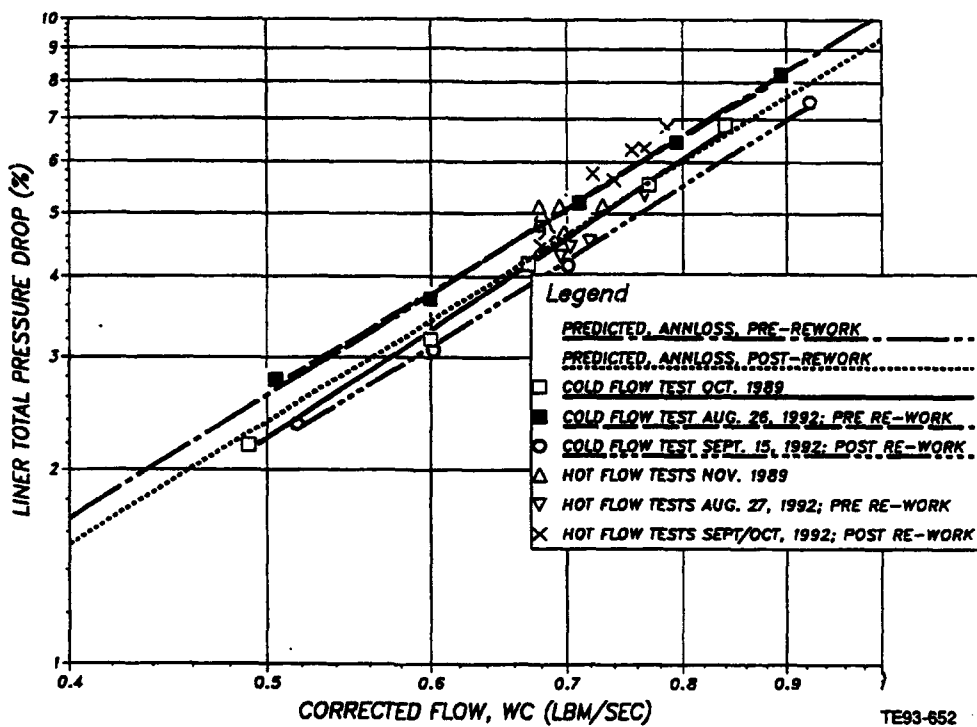


Figure 7.—Army/NASA CME combustor predicted and measured pressure drop versus corrected flow.

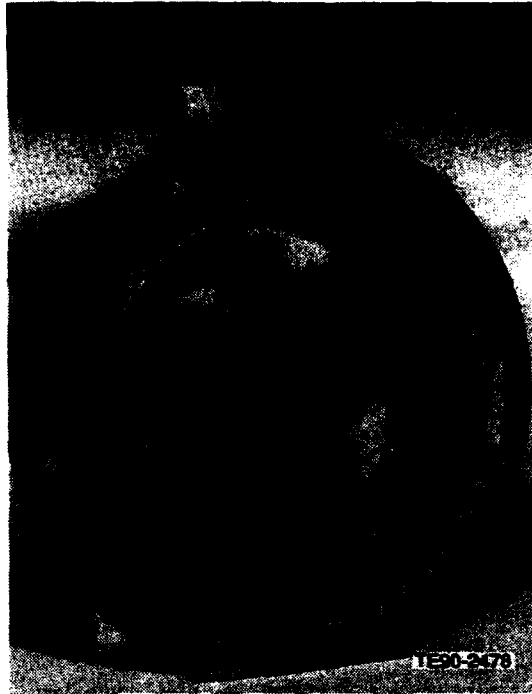


Figure 8.—CME combustor after 1989 BU1 thermal paint test.

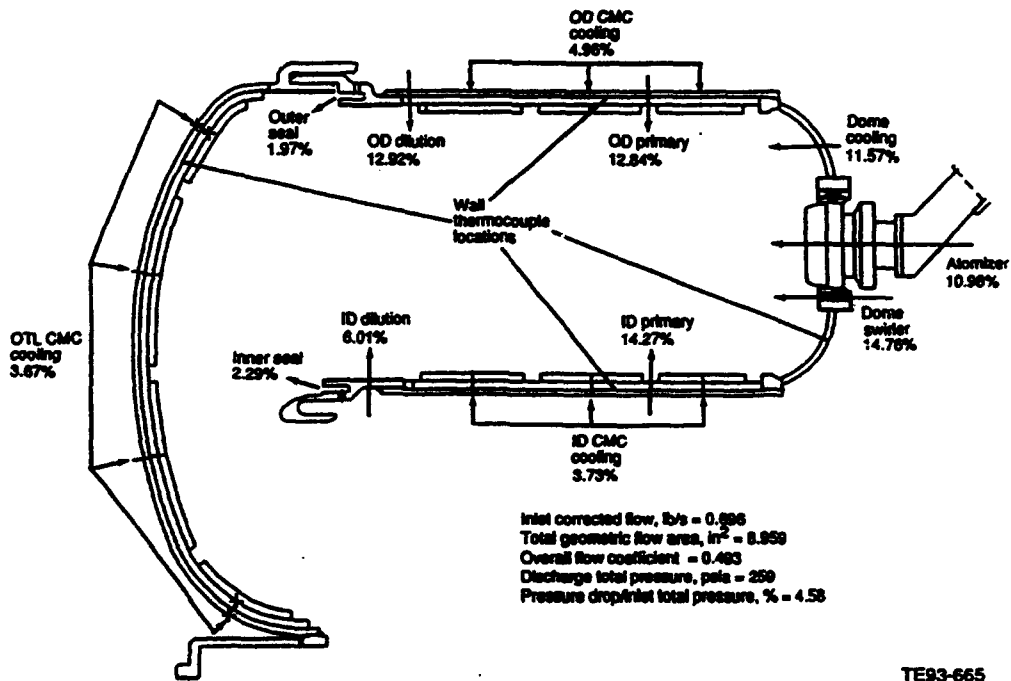


Figure 9.—CME combustor predicted airflow distribution at design point—after rework.

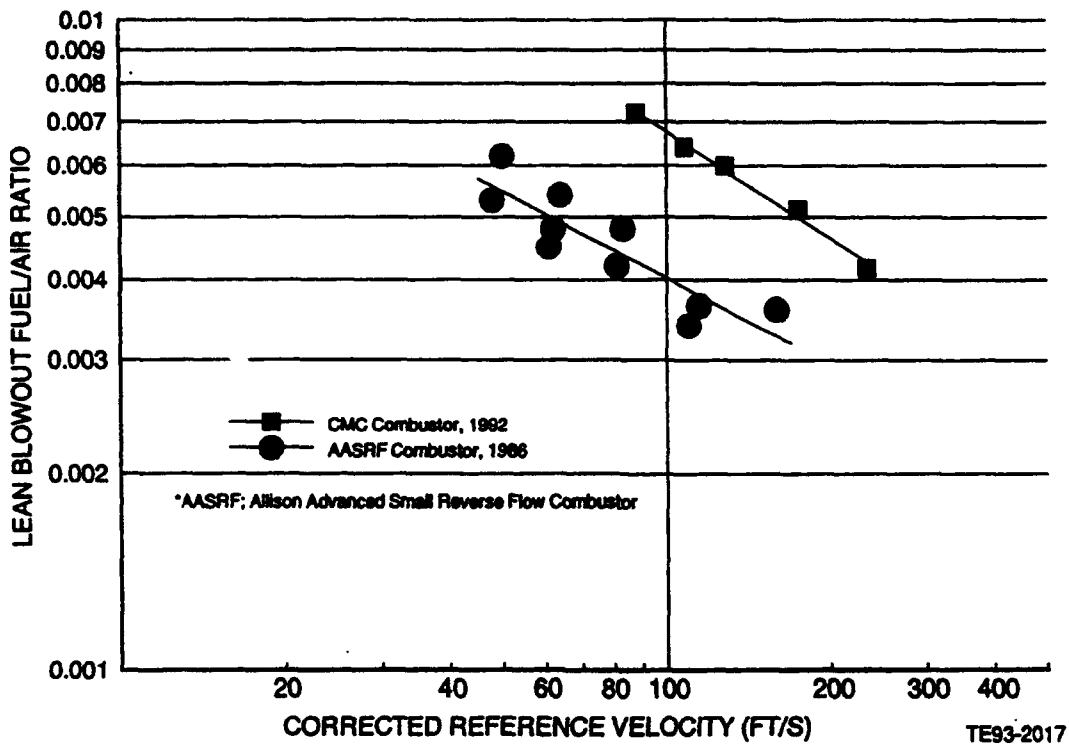


Figure 10.—CME combustor lean blowout characteristics.

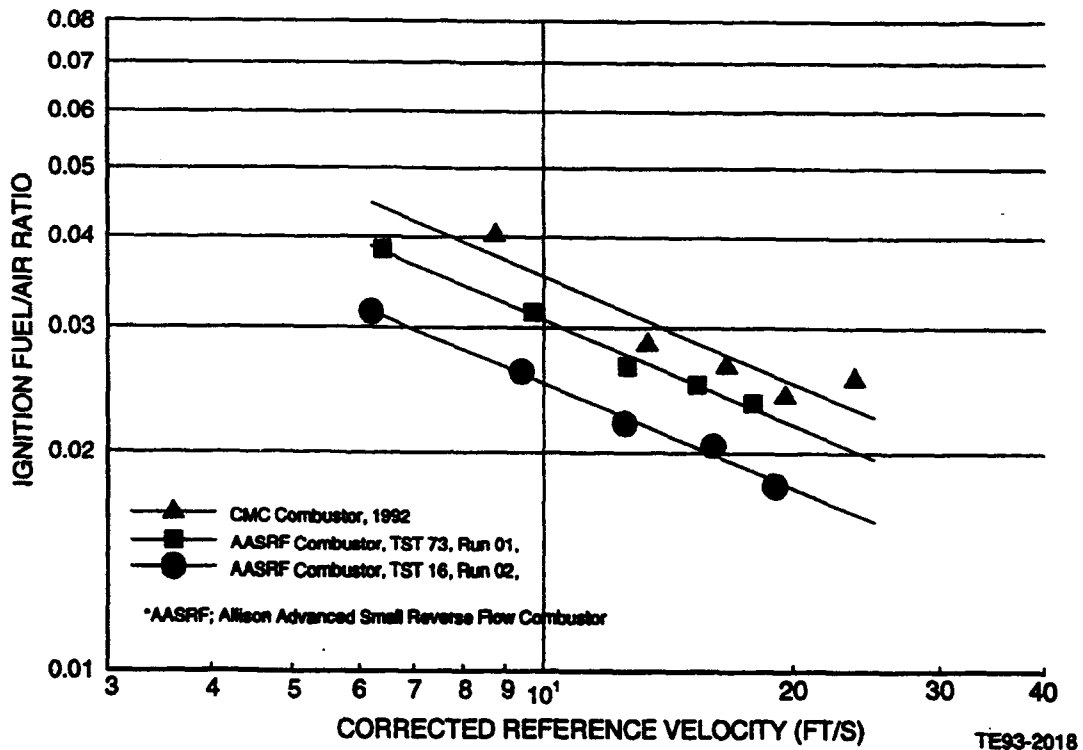


Figure 11.—CME combustor ignition characteristics.

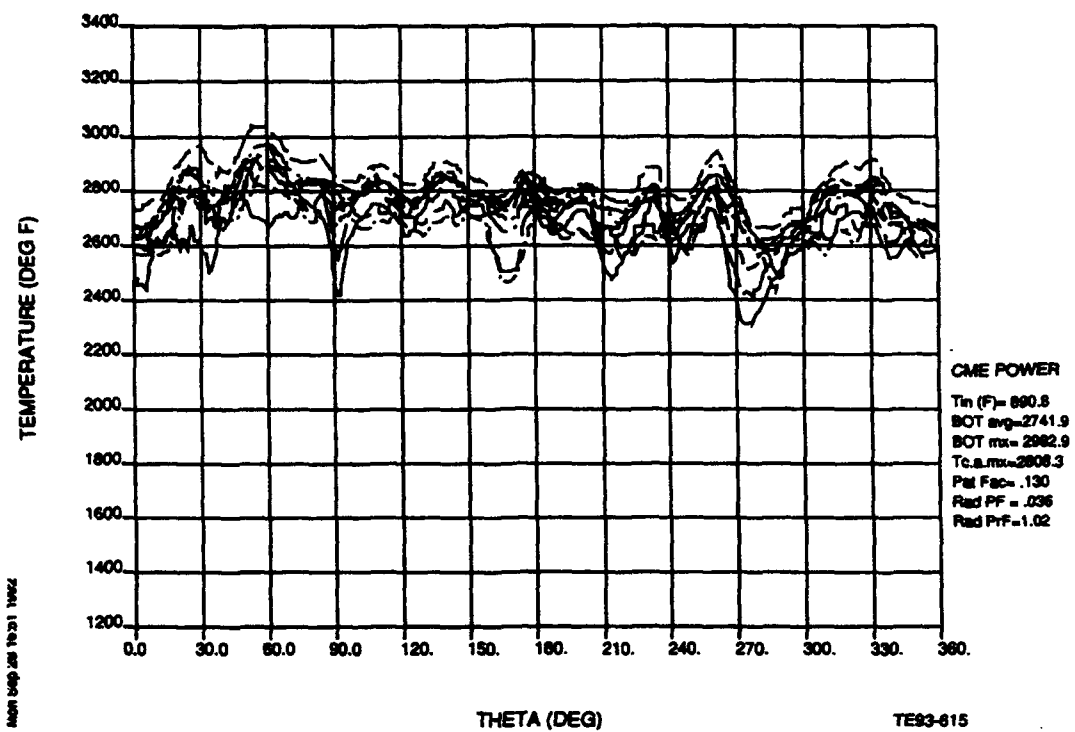


Figure 12.—Circumferential temperature trace at 2800 °F (1811K) burner outlet temperature steady-state condition.

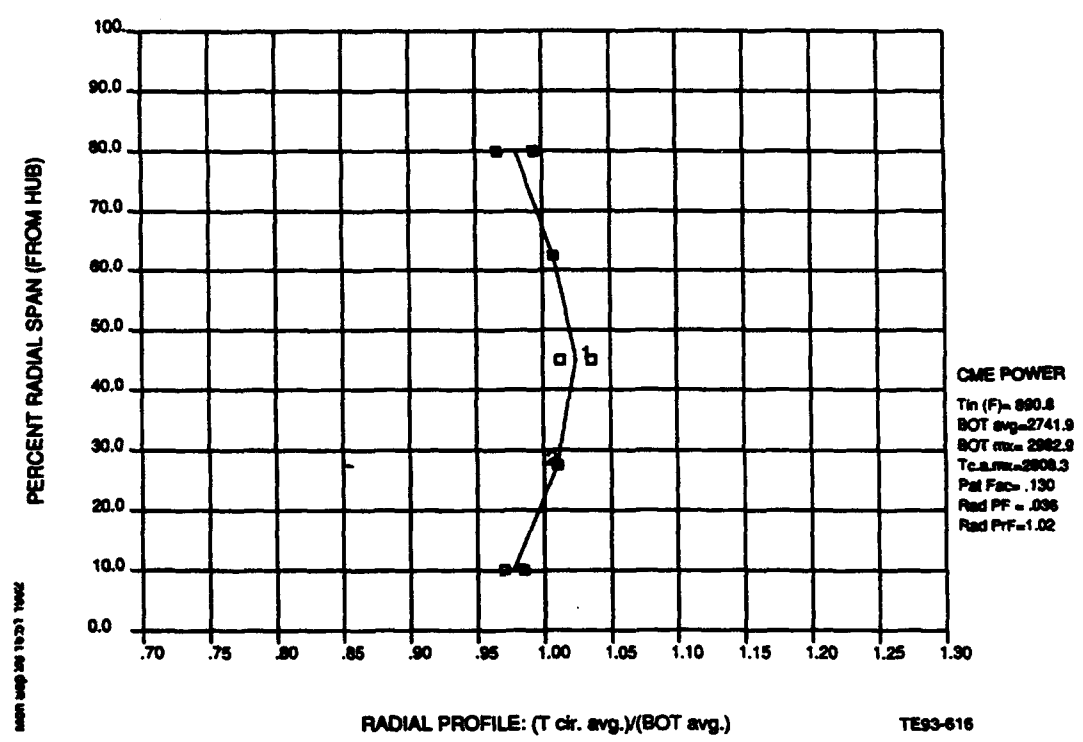


Figure 13.—Radial temperature profile at 2800 °F (1811K) burner outlet temperature steady-state condition.

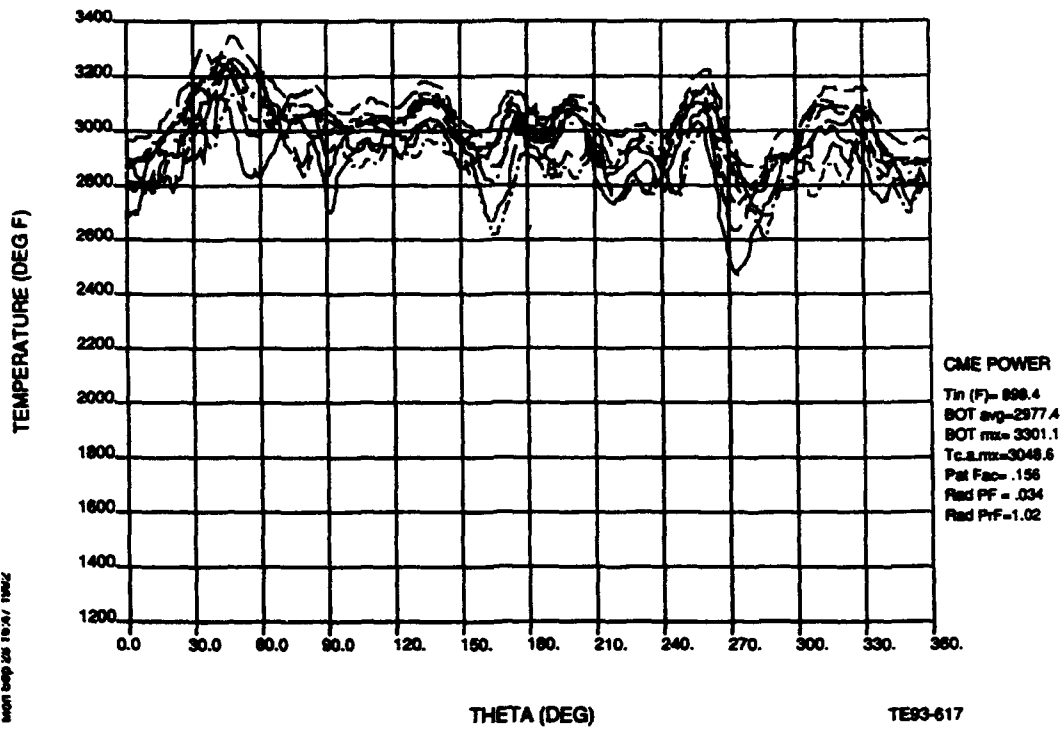


Figure 14.—Circumferential temperature trace at 3000 °F (1922K) burner outlet temperature steady-state condition.

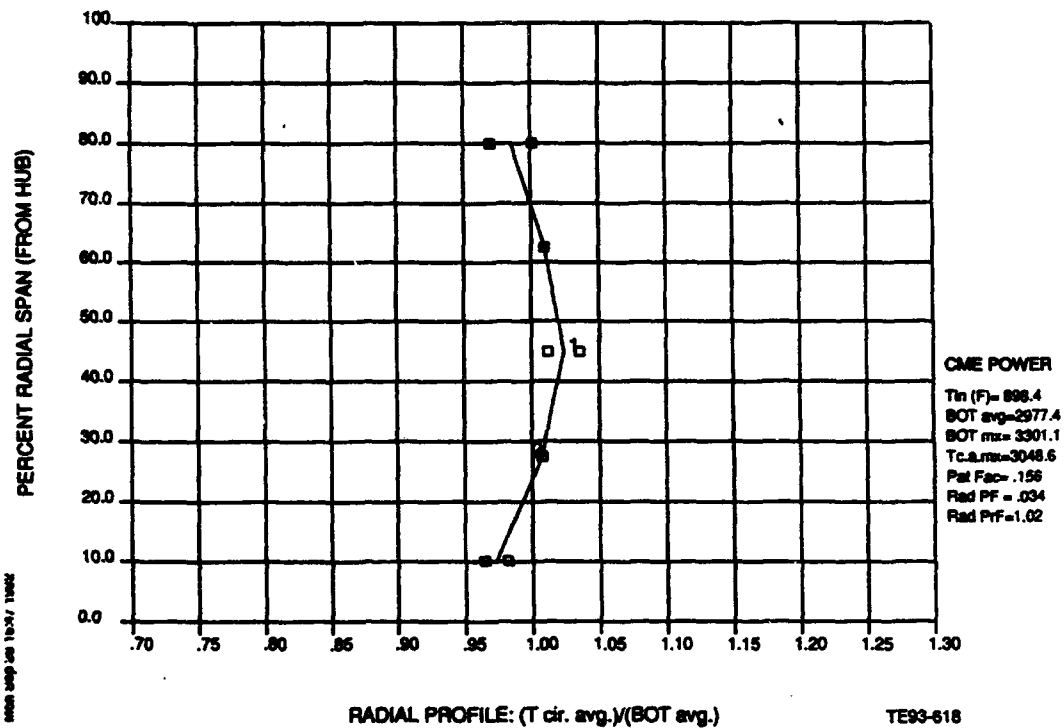


Figure 15.—Radial temperature profile at 3000 °F (1922K) burner outlet temperature steady-state condition.

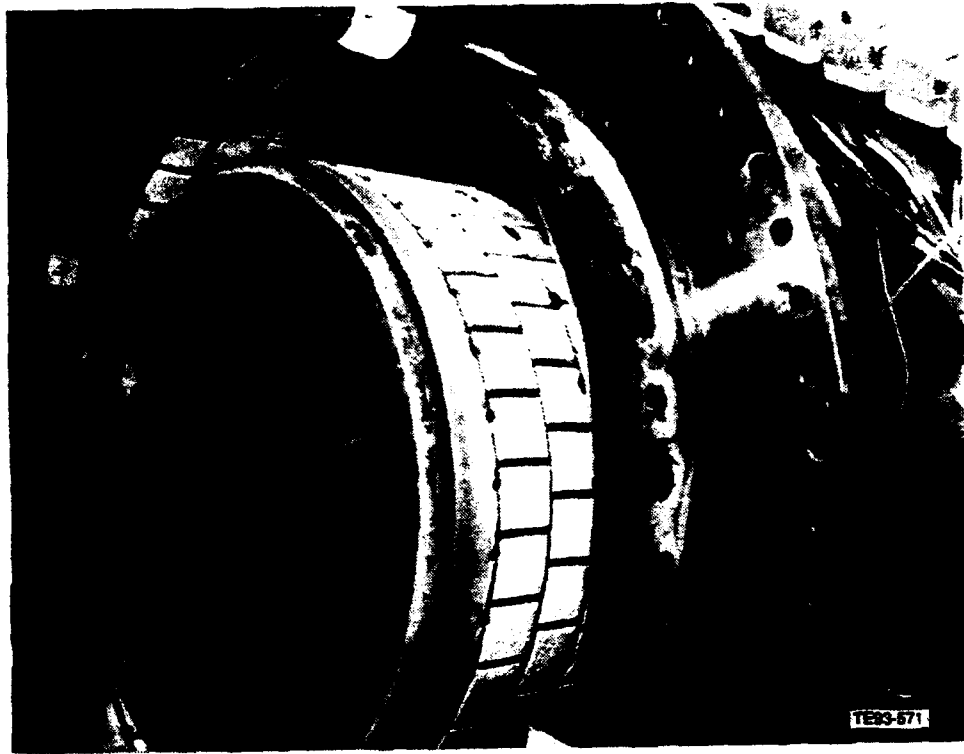


Figure 16.—CME combustor after 9/29/92 2700 °F BOT cyclic shock test—liner.

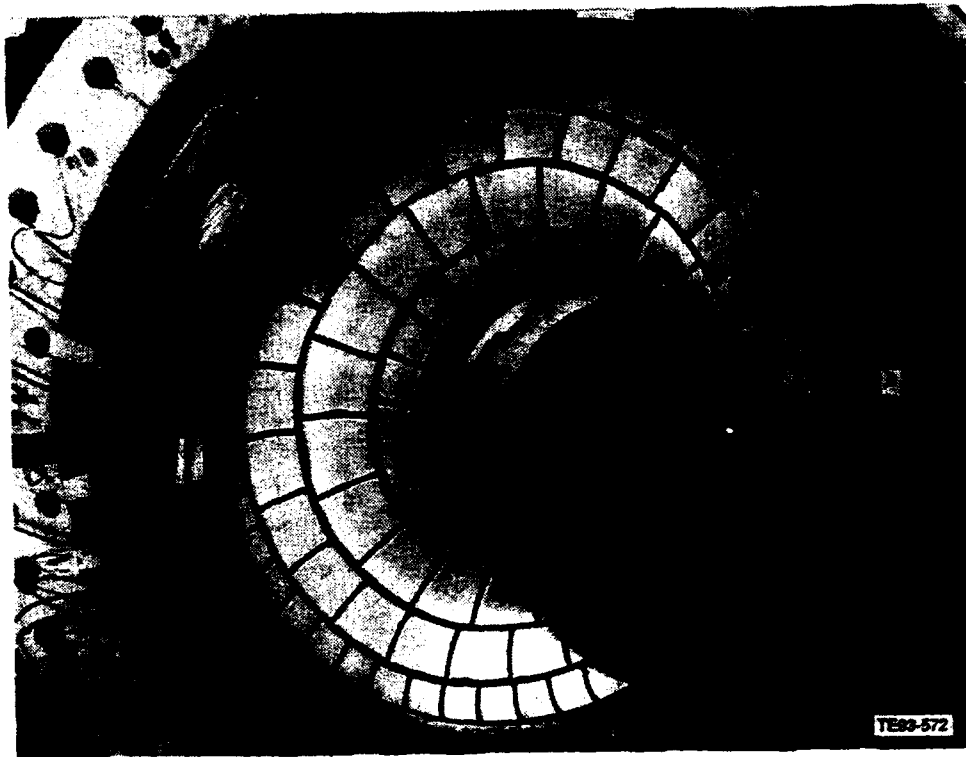


Figure 17.—CME combustor after 9/29/92 2700 °F BOT cyclic shock test—OTL.

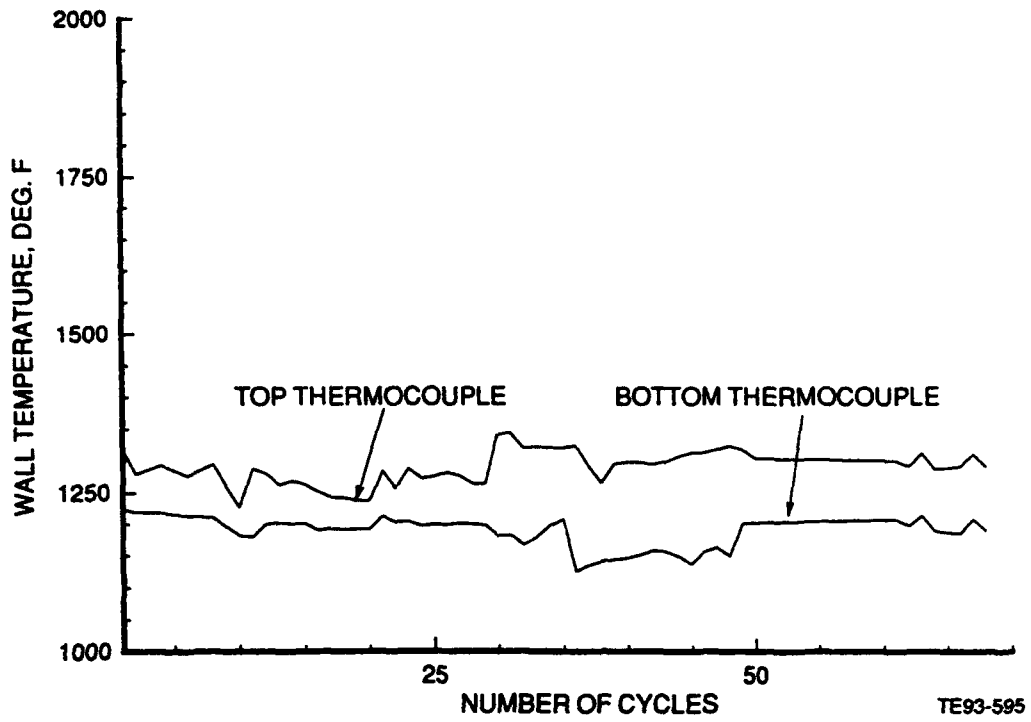


Figure 18.—Army/NASA CME combustor thermal shock test—3000 °F BOT high point, ceramic/Bransbond interface, outer barrel.

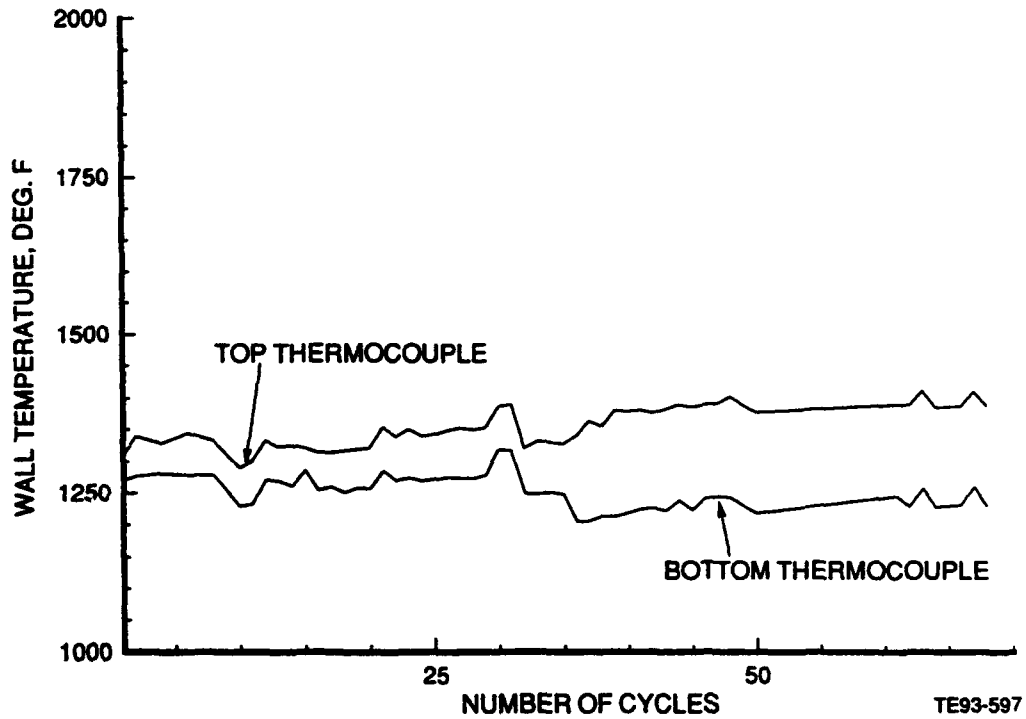


Figure 19.—Army/NASA CME combustor thermal shock test—3000 °F BOT high point, ceramic/Bransbond interface, OTL.

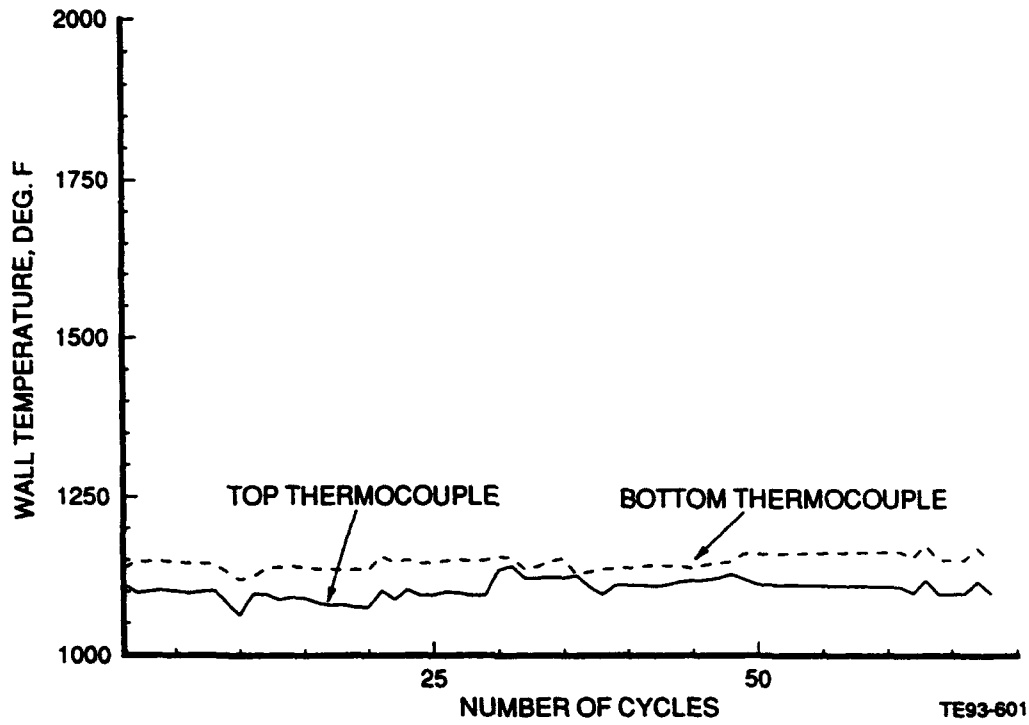


Figure 20.—Army/NASA CME combustor thermal shock test—3000 °F BOT high point, metal cold side, outer barrel.

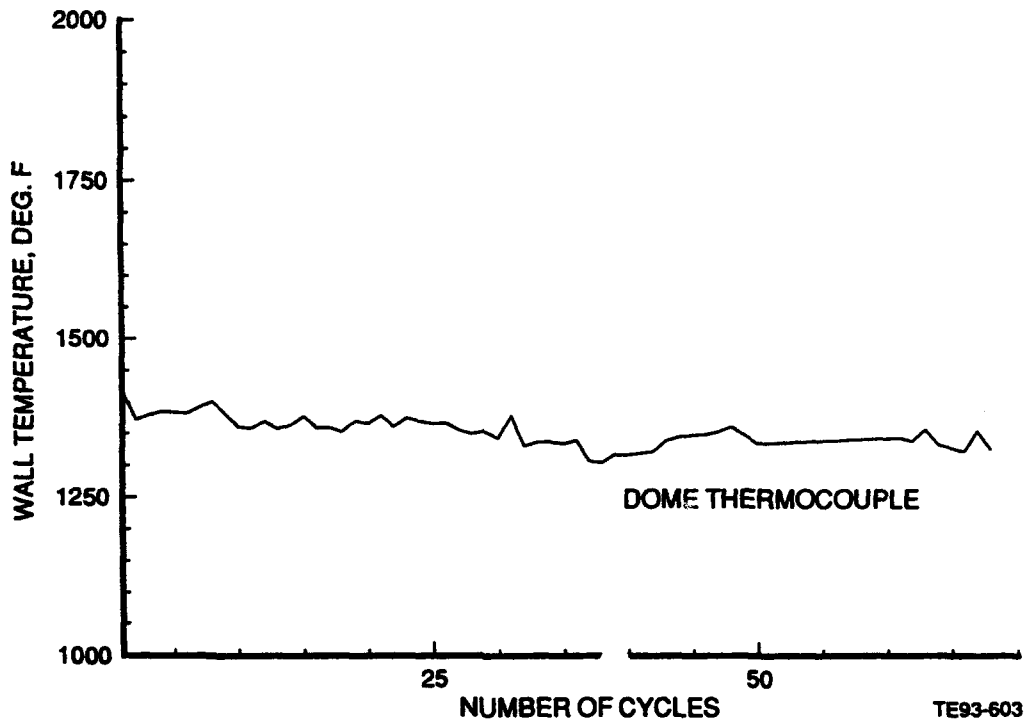


Figure 21.—Army/NASA CME combustor thermal shock test—3000 °F BOT high point, metal cold side, dome.

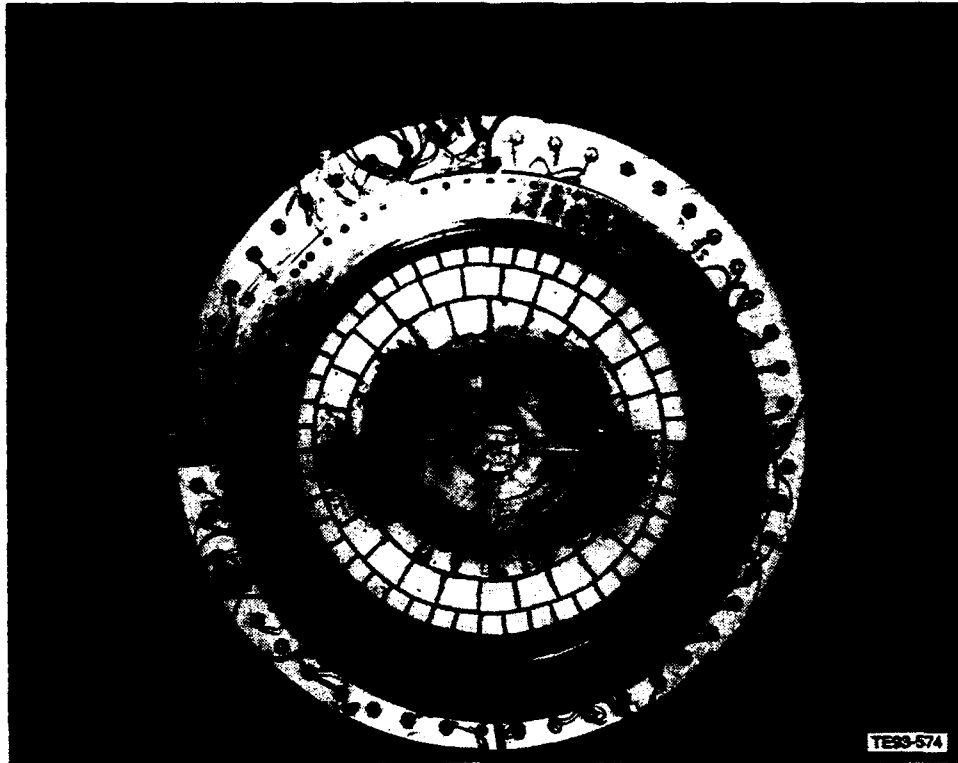


Figure 22.—CME combustor after 10/02/92 3000 °F BOT cyclic shock test—OTL.

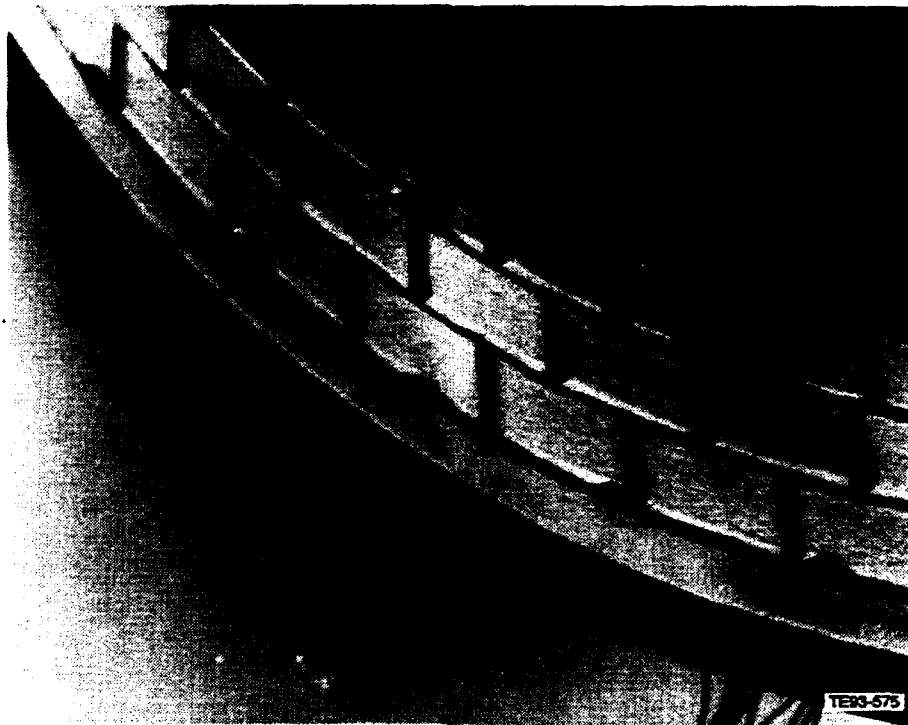


Figure 23.—CME combustor outer wall after 10/02/92 3000 °F BOT cyclic shock test.

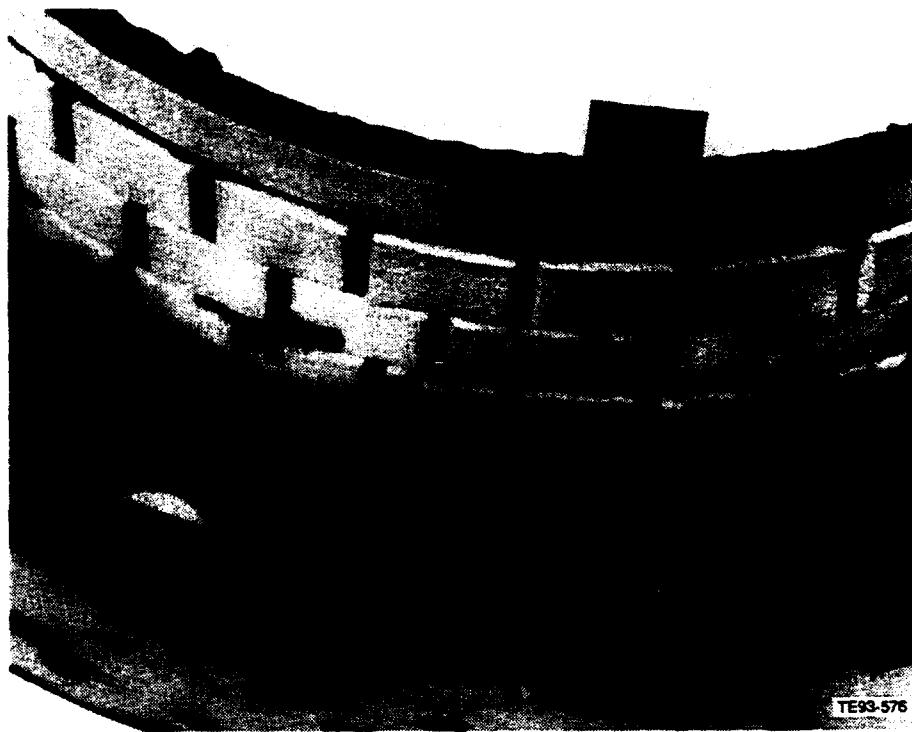


Figure 24.—CME combustor inner wall after 10/02/92 3000 °F BOT cyclic shock test.

# REPORT DOCUMENTATION PAGE

Form Approved  
OMB No. 0704-0188

Public reporting burden for this collection of information is estimated to average 1 hour per response, including the time for reviewing instructions, searching existing data sources, gathering and maintaining the data needed, and completing and reviewing the collection of information. Send comments regarding this burden estimate or any other aspect of this collection of information, including suggestions for reducing this burden, to Washington Headquarters Services, Directorate for Information Operations and Reports, 1215 Jefferson Davis Highway, Suite 1204, Arlington, VA 22202-4302, and to the Office of Management and Budget, Paperwork Reduction Project (0704-0188), Washington, DC 20503.

<b>1. AGENCY USE ONLY (Leave blank)</b>		<b>2. REPORT DATE</b> June 1994	<b>3. REPORT TYPE AND DATES COVERED</b> Technical Memorandum	
<b>4. TITLE AND SUBTITLE</b> Compliant Metal Enhanced Convection Cooled Reverse-Flow Annular Combustor			<b>5. FUNDING NUMBERS</b>  WU-537-04-20 1L162211A47A	
<b>6. AUTHOR(S)</b>  Marc D. Paskin and Waldo A. Acosta				
<b>7. PERFORMING ORGANIZATION NAME(S) AND ADDRESS(ES)</b> NASA Lewis Research Center Cleveland, Ohio 44135-3191 and Vehicle Propulsion Directorate U.S. Army Research Laboratory Cleveland, Ohio 44135-3191			<b>8. PERFORMING ORGANIZATION REPORT NUMBER</b>  E-8917	
<b>9. SPONSORING/MONITORING AGENCY NAME(S) AND ADDRESS(ES)</b> National Aeronautics and Space Administration Washington, D.C. 20546-0001 and U.S. Army Research Laboratory Adelphi, Maryland 20783-1145			<b>10. SPONSORING/MONITORING AGENCY REPORT NUMBER</b>  NASA TM-106626 ARL-MR-151 AIAA-94-2710	
<b>11. SUPPLEMENTARY NOTES</b> Prepared for the 30th Joint Propulsion Conference cosponsored by AIAA, ASME, SAE, and ASEE, Indianapolis, Indiana, June 27-29, 1994. Marc D. Paskin, Allison Engine Co., P.O. Box 420, Indianapolis, Indiana 46206 (work funded by NASA Contract NAS3-24226) and Waldo A. Acosta, Vehicle Propulsion Directorate, U.S. Army Research Laboratory, NASA Lewis Research Center. Responsible person, Waldo A. Acosta, organization code 5102, (216) 433-3393.				
<b>12a. DISTRIBUTION/AVAILABILITY STATEMENT</b>  Unclassified - Unlimited Subject Category 07			<b>12b. DISTRIBUTION CODE</b>	
<b>13. ABSTRACT (Maximum 200 words)</b>  A joint Army/NASA program was conducted to design, fabricate, and test an advanced, reverse-flow, small gas turbine combustor using a compliant metal enhanced (CME) convection wall cooling concept. The objectives of this effort were to develop a design method (basic design data base and analysis) for the CME cooling technique and then demonstrate its application to an advanced cycle, small, reverse-flow combustor with 3000°F (1922 K) burner outlet temperature (BOT). The CME concept offers significant improvements in wall cooling effectiveness resulting in a large reduction in cooling air requirements. Therefore, more air is available for control of burner outlet temperature pattern in addition to the benefits of improved efficiency, reduced emissions, and smoke levels. Rig test results demonstrated the benefits and viability of the CME concept meeting or exceeding the aerothermal performance and liner wall temperature characteristics of similar lower temperature-rise combustors, achieving 0.15 pattern factor at 3000°F (1922 K) BOT, while utilizing approximately 80% less cooling air than conventional, film-cooled combustion systems.				
<b>14. SUBJECT TERMS</b> Combustor; Compliant layer; Linear cooling; Gas turbine; Thermal barrier coating; Ceramics			<b>15. NUMBER OF PAGES</b> 26	
			<b>16. PRICE CODE</b> A03	
<b>17. SECURITY CLASSIFICATION OF REPORT</b> Unclassified	<b>18. SECURITY CLASSIFICATION OF THIS PAGE</b> Unclassified	<b>19. SECURITY CLASSIFICATION OF ABSTRACT</b> Unclassified	<b>20. LIMITATION OF ABSTRACT</b>	